

Supporting information

Unveiling the mechanism of CO₂ electroreduction to C₁ and C₂ products on ordered double transition metal MXenes.

Romana Khanam^a, Syed Fozia^a and Manzoor Ahmad Dar^{a*}

^a Department of Chemistry, Islamic University of Science and Technology,

Awantipora, Jammu and Kashmir-192122, India

Table of Contents

Table S1: Optimized geometries of Unit cells of M-Xenes along with calculated lattice parameters.

Fig. S1: Top view of optimised structures of M'₂M''C M-Xenes where M' can be Cr, Mo, Ti, V and M'' be Nb, Ta, Ti, and V.

Fig. S2: Top view of lowest energy configuration of CO₂ adsorbed on M-Xenes.

Table S2: Calculated Bader charge of CO₂ adsorbed on MXenes.

Table S3: Calculated activation barrier of C-O dissociation mechanism for three best catalysts.

Fig. S3: Phase plot comparing CO₂ binding energy with a) binding energy of *OH b) binding energy of *H c) binding energy of *O

Fig. S4: Behaviour of CO₂ adsorption on the catalyst surface with other co-adsorbates (*H, *O, *OH).

Fig. S5: Detailed computed free energy diagram representing the various possible pathways for the reduction of CO₂ to C₁ products on **a)** Cr₂NbC₂ **b)** Cr₂TaC₂ **c)** Cr₂TiC₂ **d)** Cr₂VC₂ **e)** Mo₂NbC₂ **f)** Mo₂TaC₂ **g)** Mo₂TiC₂ **h)** Mo₂VC₂ **i)** Ti₂NbC₂ **j)** Ti₂TaC₂ **k)** V₂TaC₂ **l)** V₂TiC₂

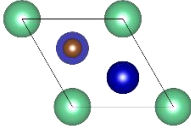
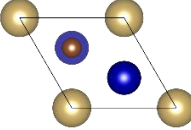
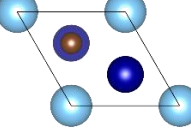
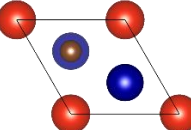
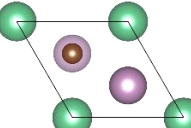
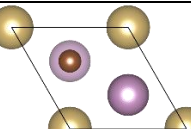
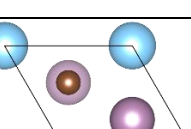
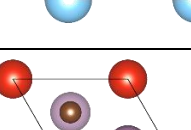
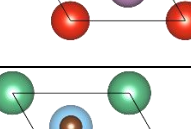
Fig. S6: Detailed computed free energy diagram representing the various possible pathways for the reduction of CO₂ to C₂ products on **a)** Cr₂NbC₂ **b)** Cr₂TaC₂ **c)** Cr₂TiC₂ **d)** Cr₂VC₂ **e)** Mo₂NbC₂ **f)** Mo₂TaC₂ **g)** Mo₂TiC₂ **h)** Mo₂VC₂ **i)** Ti₂NbC₂ **j)** Ti₂TaC₂ **k)** V₂TaC₂ **l)** V₂TiC₂

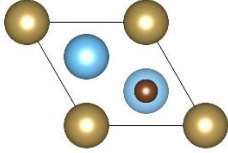
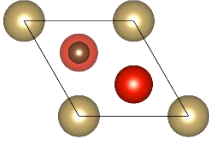
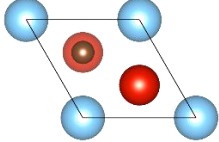
Fig. S7: Proposed reaction mechanism for CO₂ reduction to **a)** C₁ products (CH₄ and CH₃OH) and **b)** C₂ products (C₂H₄ and C₂H₅OH) on MXenes.

Fig S8: Electrode/Solution Interface of potential determining steps of CO₂ reduction on Mo₂TaC₂ MXene: **a)** Initial state and **b)** Final state of C₂ products.

Fig. S9: Variation of energy versus the AIMD simulation time for Mo_2TaC_2 for 6 ps at 600 K. The insets are the top views of snapshots of configurations.

Table S1: *Optimized geometries of Unit cells of M-Xenes along with calculated lattice parameters.*

System	Structure	Lattice parameters
Cr_2NbC_2		$a=b=3.175 \text{ \AA}$ $c=5.874 \text{ \AA}$ $\alpha=\beta=90^\circ$ $\gamma=120^\circ$
Cr_2TaC_2		$a=b=3.164 \text{ \AA}$ $c=5.816 \text{ \AA}$ $\alpha=\beta=90^\circ$ $\gamma=120^\circ$
Cr_2TiC_2		$a=b=3.035 \text{ \AA}$ $c=6.242 \text{ \AA}$ $\alpha=\beta=90^\circ$ $\gamma=120^\circ$
Cr_2VC_2		$a=b=3.006 \text{ \AA}$ $c=6.172 \text{ \AA}$ $\alpha=\beta=90^\circ$ $\gamma=120^\circ$
Mo_2NbC_2		$a=b=3.282 \text{ \AA}$ $c=6.584 \text{ \AA}$ $\alpha=\beta=90^\circ$ $\gamma=120^\circ$
Mo_2TaC_2		$a=b=3.134 \text{ \AA}$ $c=7.050 \text{ \AA}$ $\alpha=\beta=90^\circ$ $\gamma=120^\circ$
Mo_2TiC_2		$a=b=3.167 \text{ \AA}$ $c=6.712 \text{ \AA}$ $\alpha=\beta=90^\circ$ $\gamma=120^\circ$
Mo_2VC_2		$a=b=3.188 \text{ \AA}$ $c=6.438 \text{ \AA}$ $\alpha=\beta=90^\circ$ $\gamma=120^\circ$
Ti_2NbC_2		$a=b=3.157 \text{ \AA}$ $c=7.143 \text{ \AA}$ $\alpha=\beta=90^\circ$ $\gamma=120^\circ$

Ti₂TaC₂		$a=b=3.089 \text{ \AA}$ $c=7.480 \text{ \AA}$ $\alpha=\beta=90^\circ$ $\gamma=120^\circ$
V₂TaC₂		$a=b=3.091 \text{ \AA}$ $c=6.681 \text{ \AA}$ $\alpha=\beta=90^\circ$ $\gamma=120^\circ$
V₂TiC₂		$a=b=3.005 \text{ \AA}$ $c=6.816 \text{ \AA}$ $\alpha=\beta=90^\circ$ $\gamma=120^\circ$

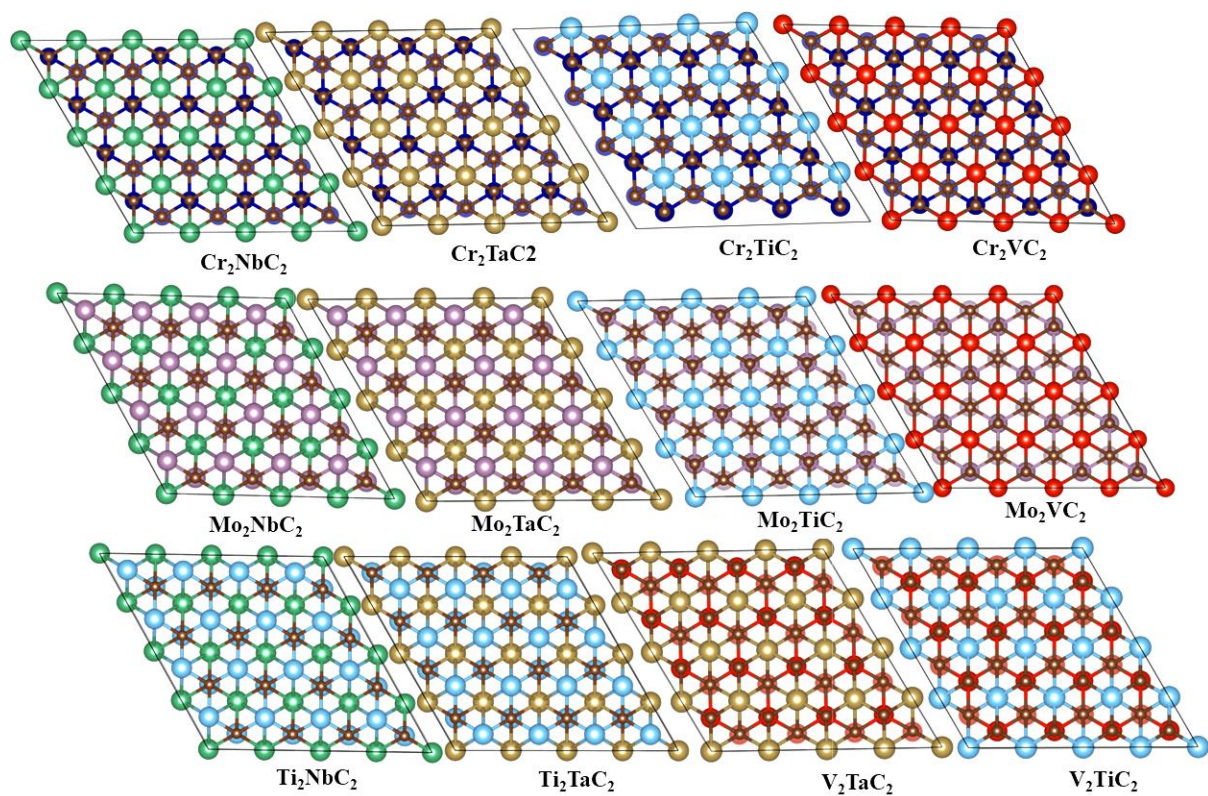


Fig S1: Top view of optimised structures of $M'_2M''C$ MXenes where M' can be Cr, Mo, Ti, V and M'' be Nb, Ta, Ti, and V.

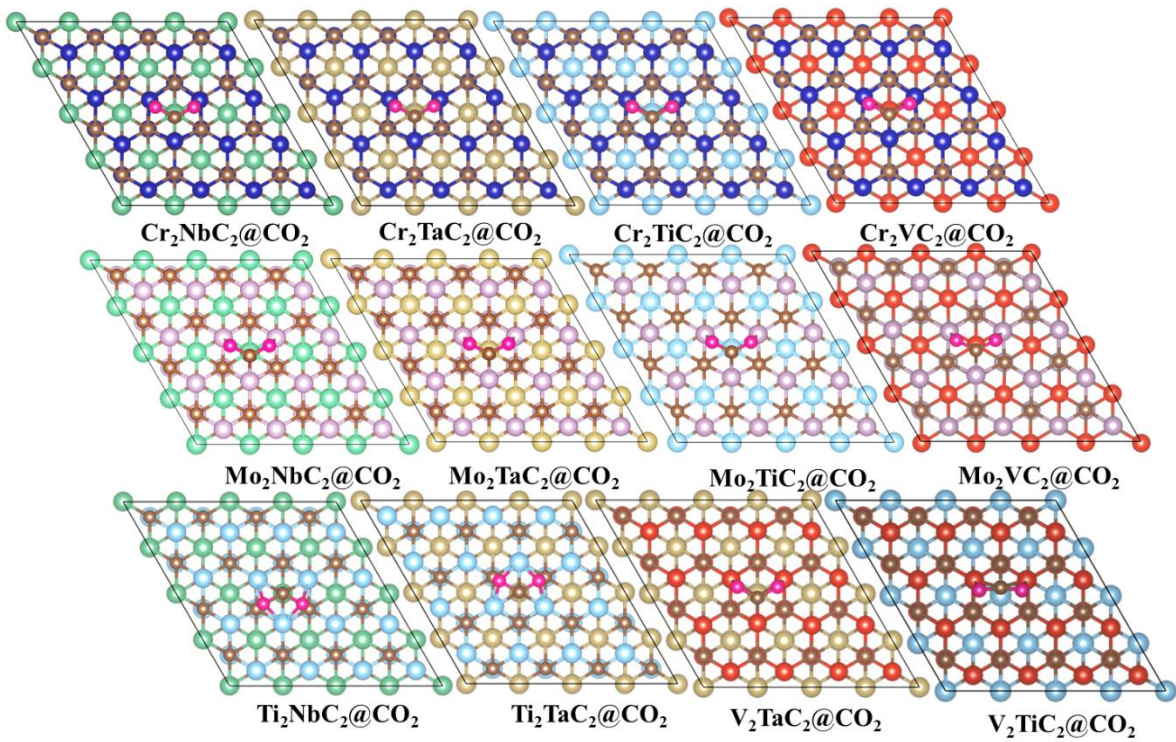


Fig. S2: Top view of lowest energy configuration of CO_2 adsorbed on MXenes.

Table S2: Calculated Bader charge of CO₂ adsorbed on MXenes.

Catalyst	C (e)	O (e)	Net Bader charge (e)
Cr ₂ NbC ₂	0.86	-1.06	-1.26
Cr ₂ TaC ₂	0.87	-1.06	-1.25
Cr ₂ TiC ₂	0.82	-1.05	-1.28
Cr ₂ VC ₂	0.82	-1.05	-1.28
Mo ₂ NbC ₂	0.87	-1.05	-1.23
Mo ₂ TaC ₂	0.87	-1.05	-1.23
Mo ₂ TiC ₂	0.88	-1.05	-1.22
Mo ₂ VC ₂	0.86	-1.06	-1.26
Ti ₂ NbC ₂	0.67	-1.13	-1.59
Ti ₂ TaC ₂	0.59	-1.12	-1.65
V ₂ TaC ₂	0.71	-1.06	-1.41
V ₂ TiC ₂	1.07	-1.12	-1.17

Table S3: Calculated activation barrier of C-O dissociation mechanism for three best catalysts.

Catalyst	ΔG_{CO} (eV)	ΔG_{CO_2} (eV)	ΔG_a (eV)
Mo ₂ TaC ₂	-1.38	-1.9	0.51
Mo ₂ TiC ₂	-1.66	-2.18	0.52
Mo ₂ VC ₂	-1.82	-2.45	0.63

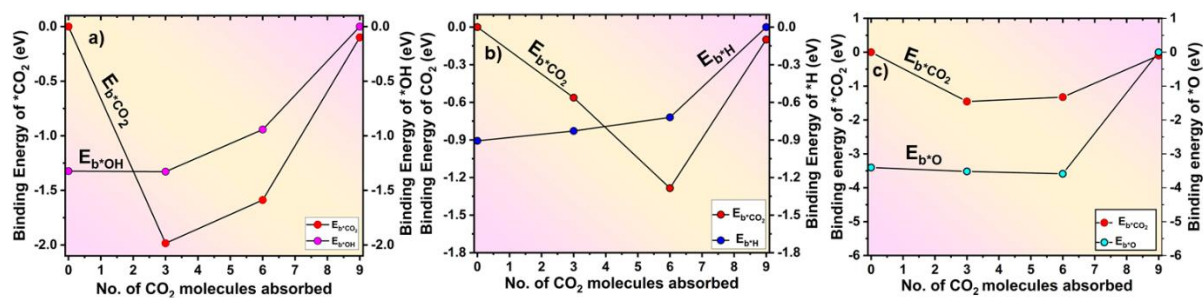


Fig. S3: Phase plot comparing CO_2 binding energy with a) binding energy of *OH b) binding energy of *H c) binding energy of *O

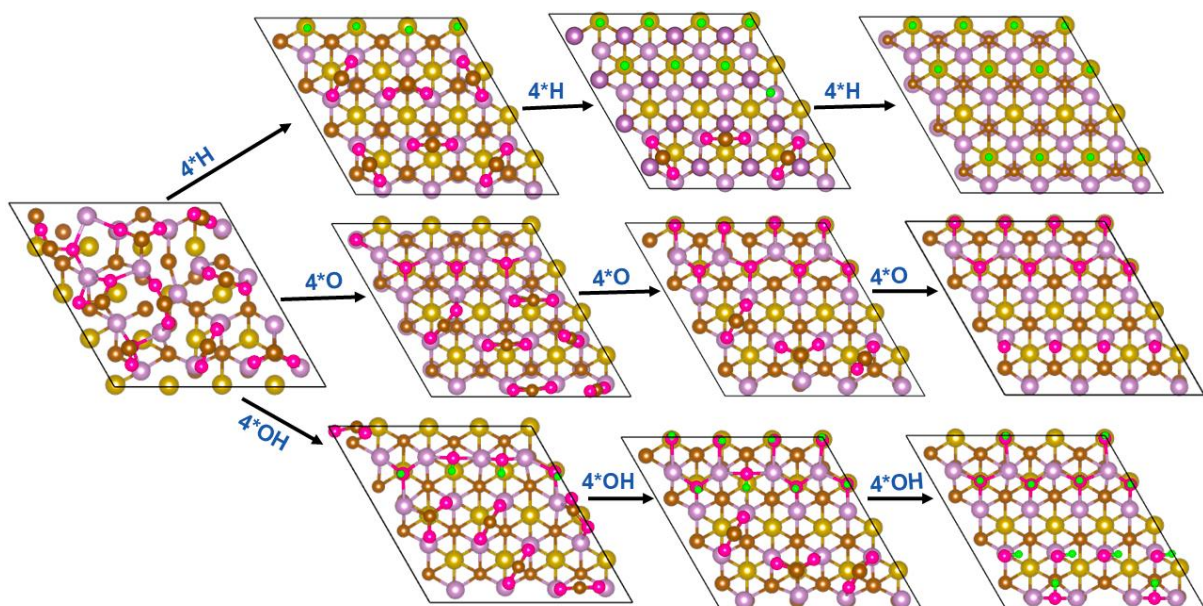
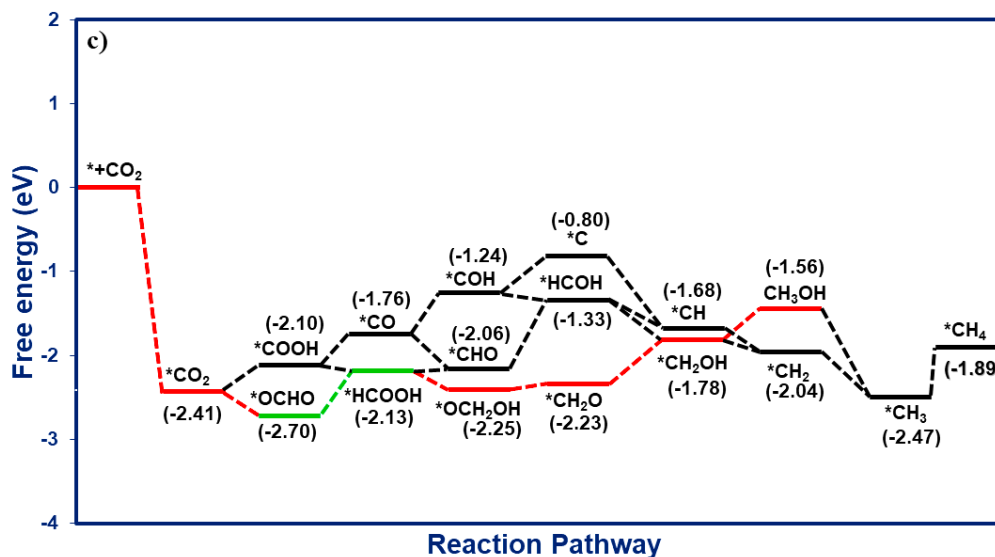
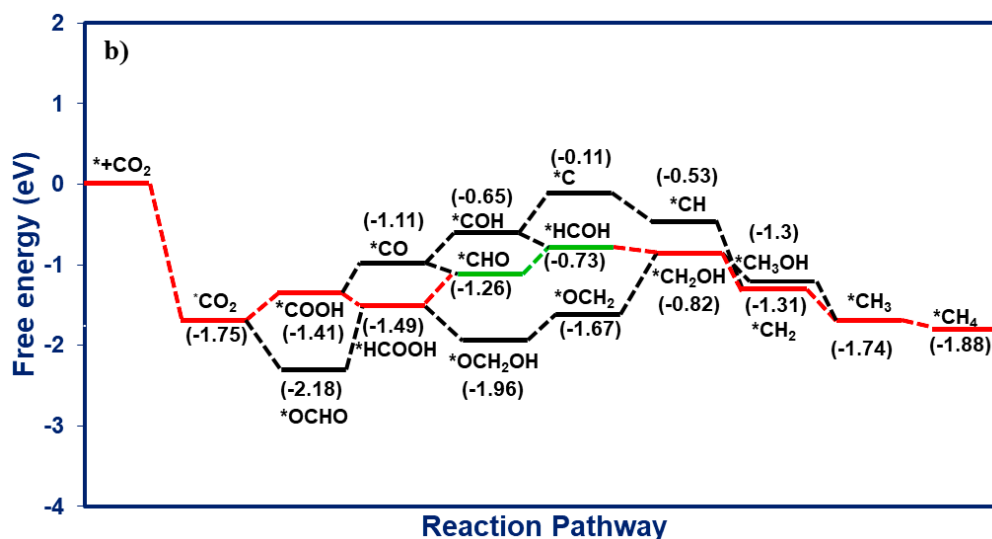
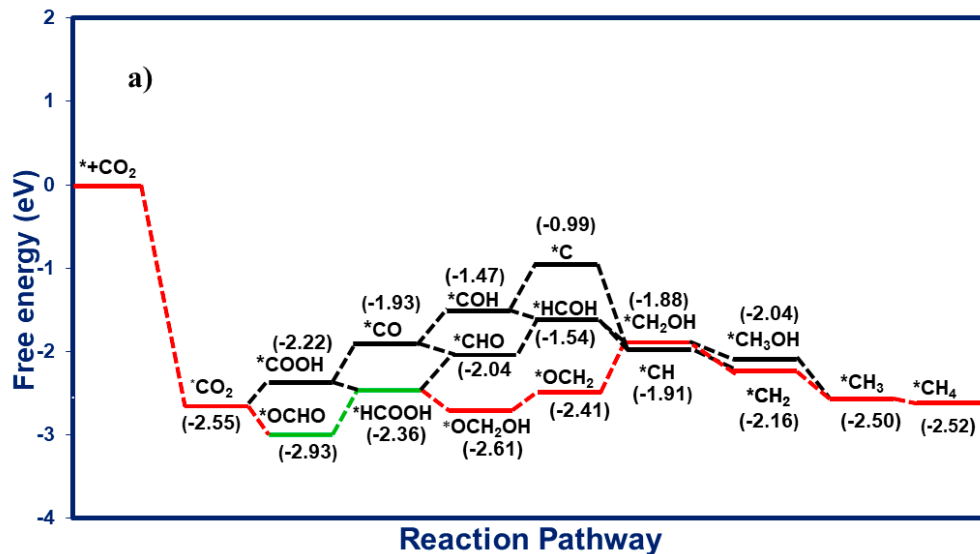
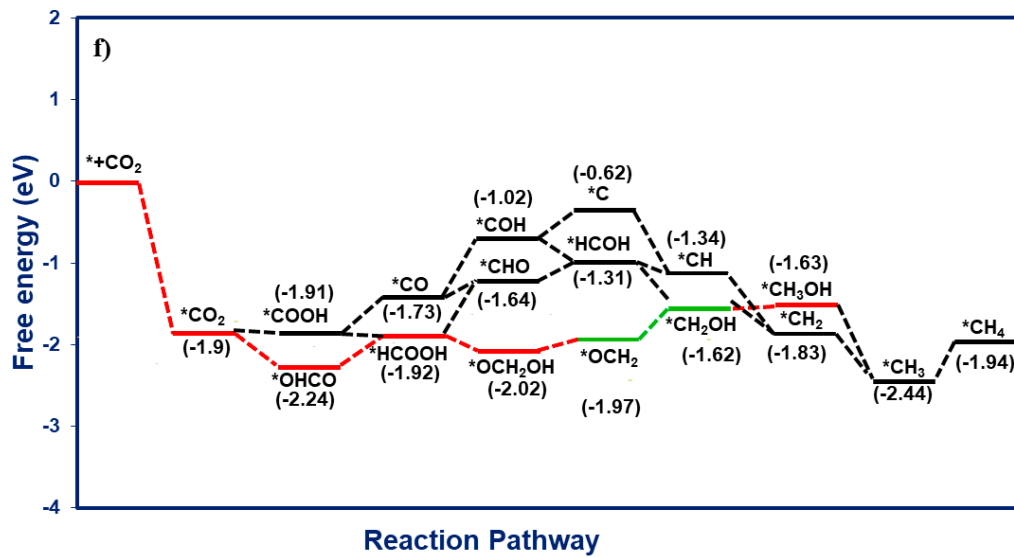
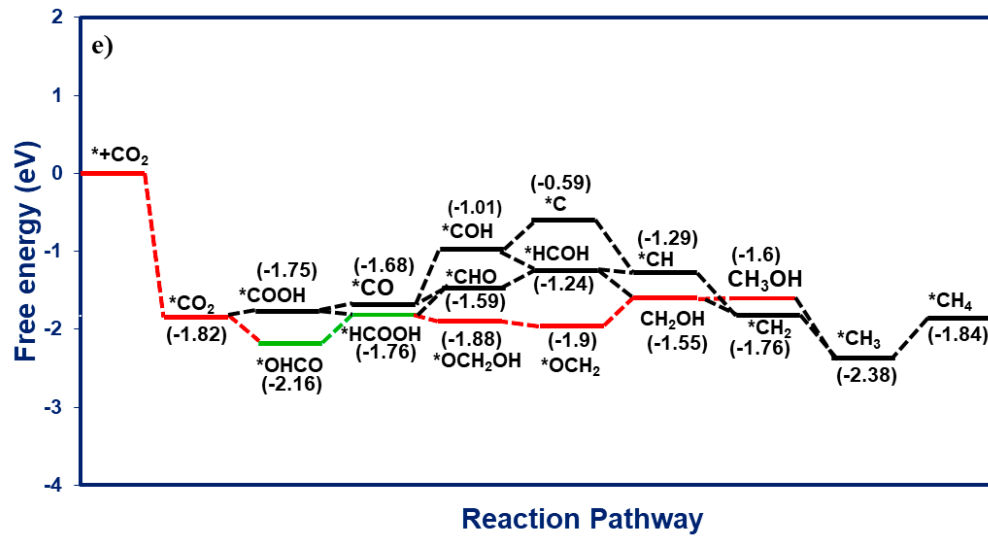
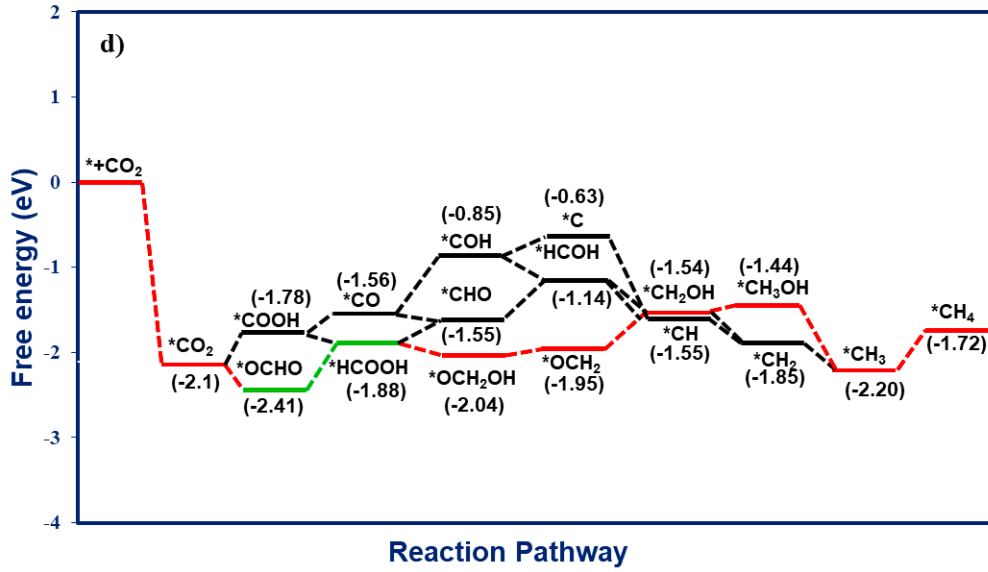
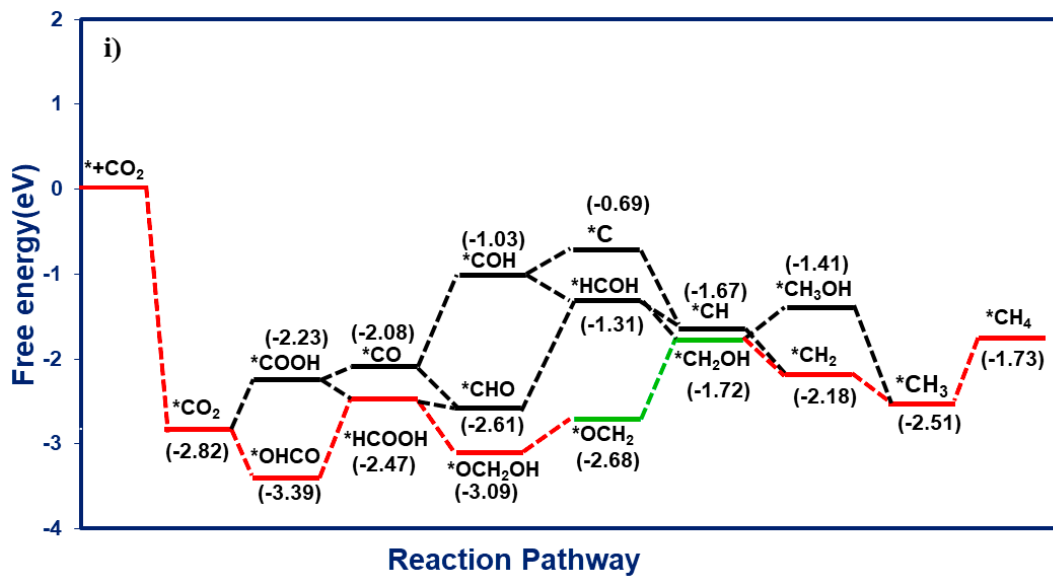
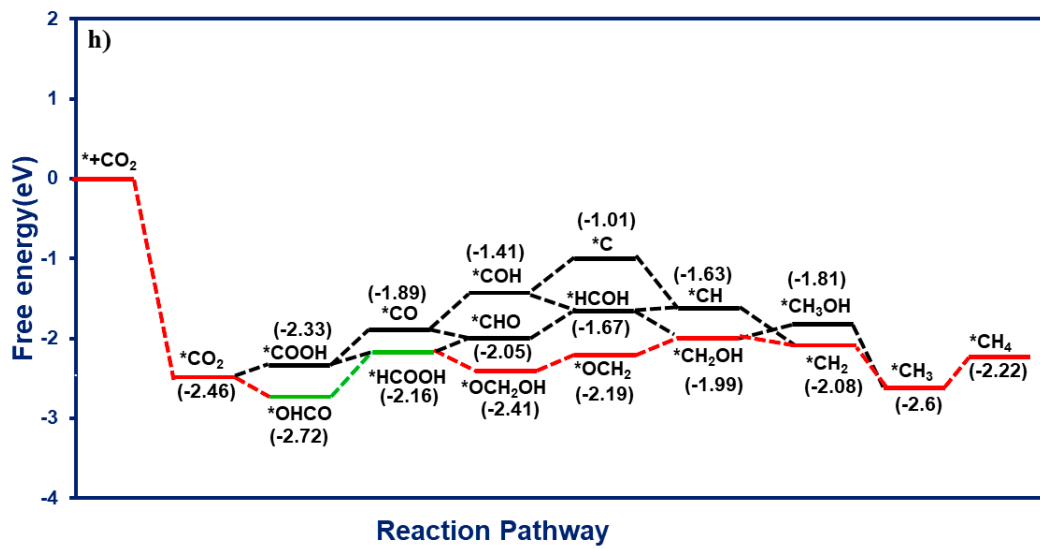
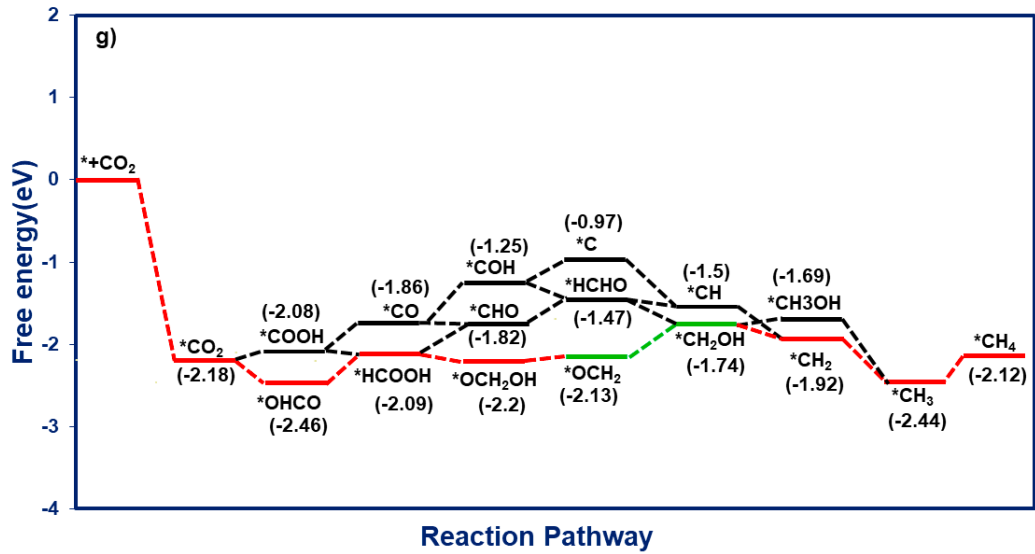


Fig. S4: Behaviour of CO_2 adsorption on the catalyst surface with other co-adsorbates (*H , *O , *OH).







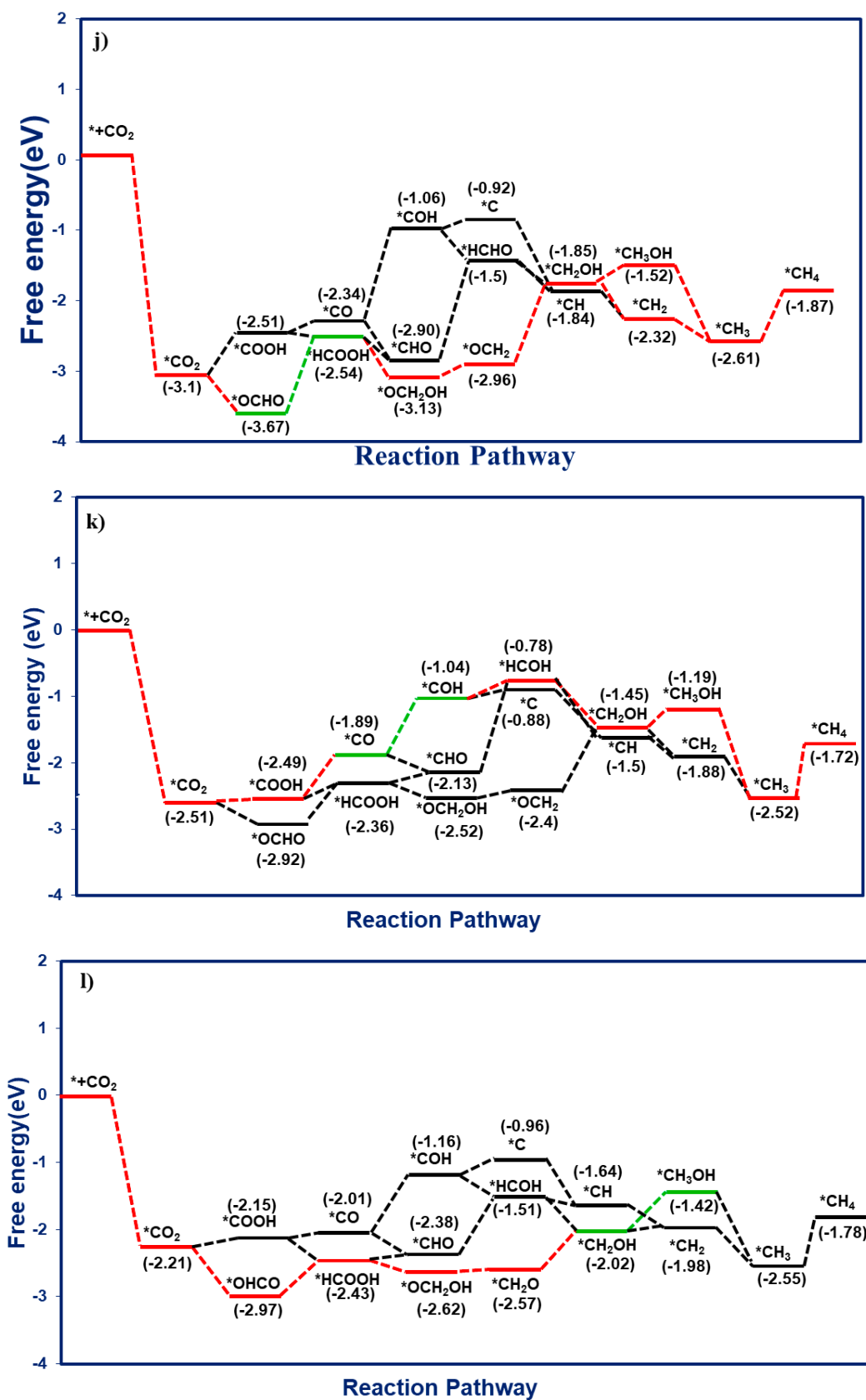
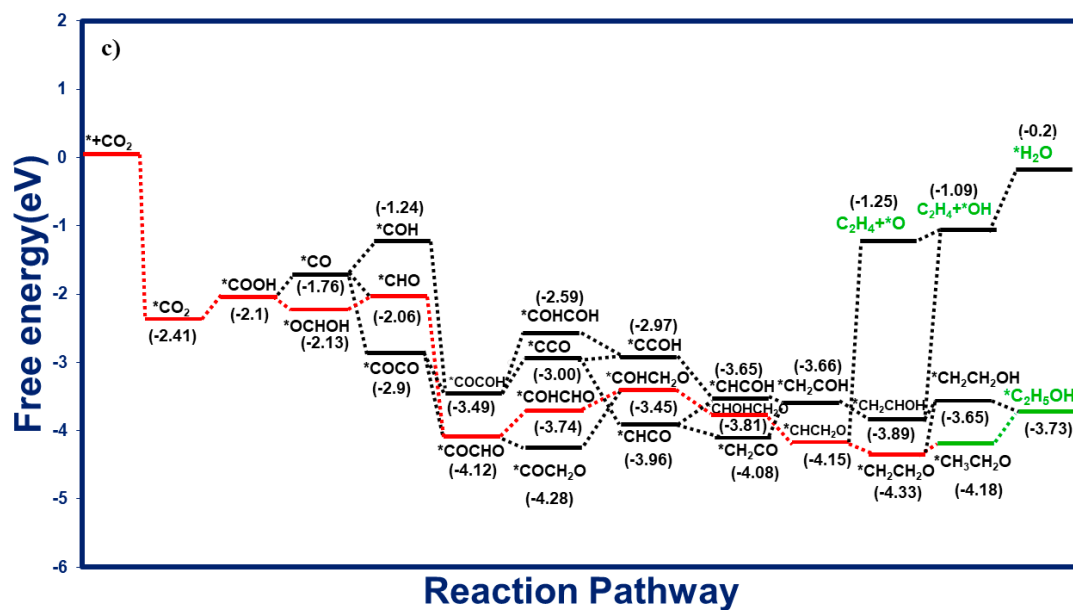
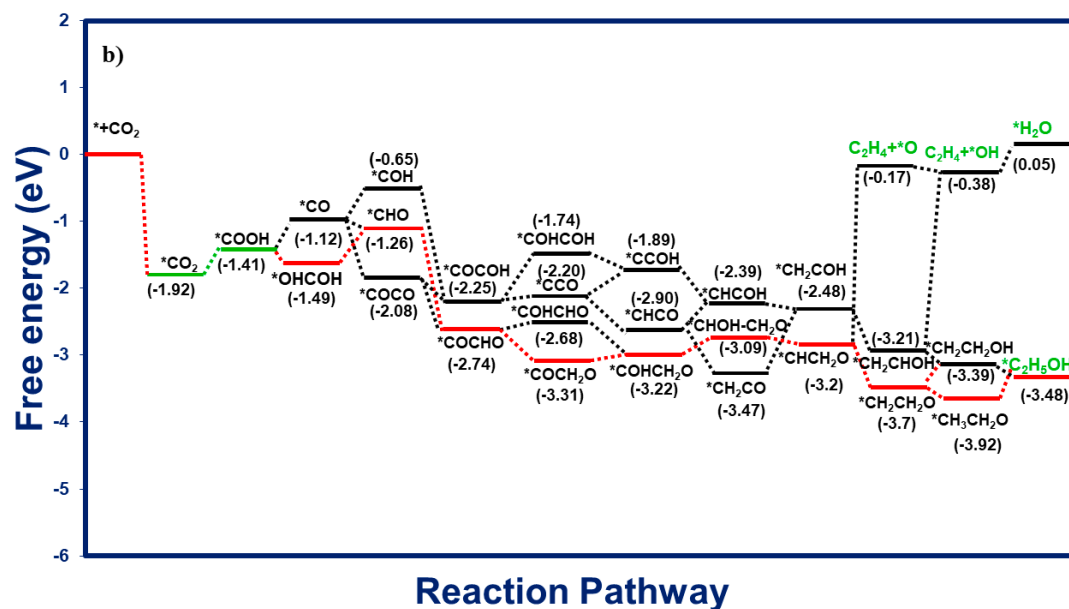
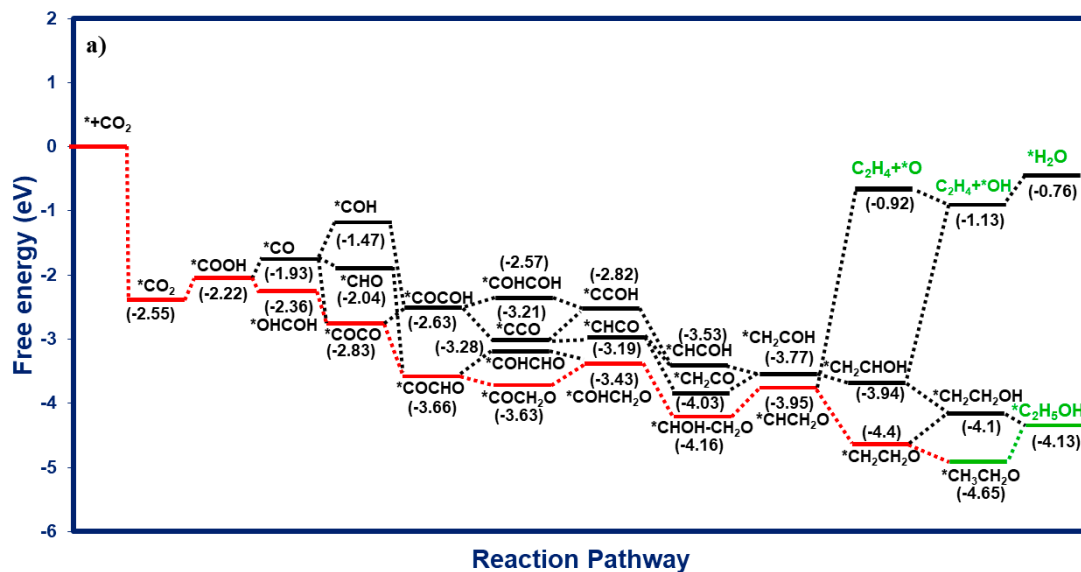
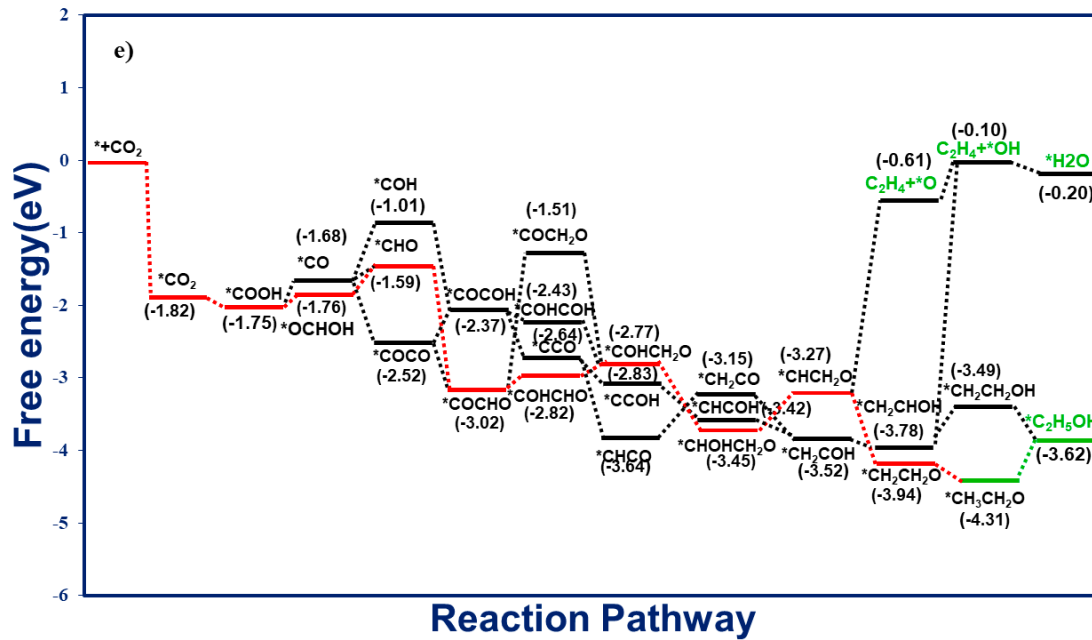
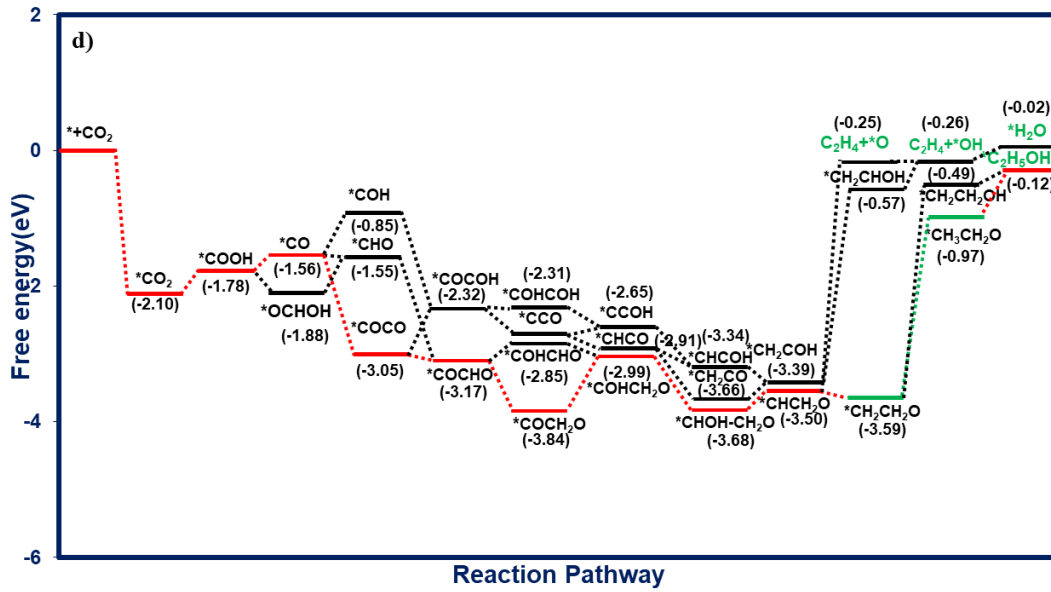
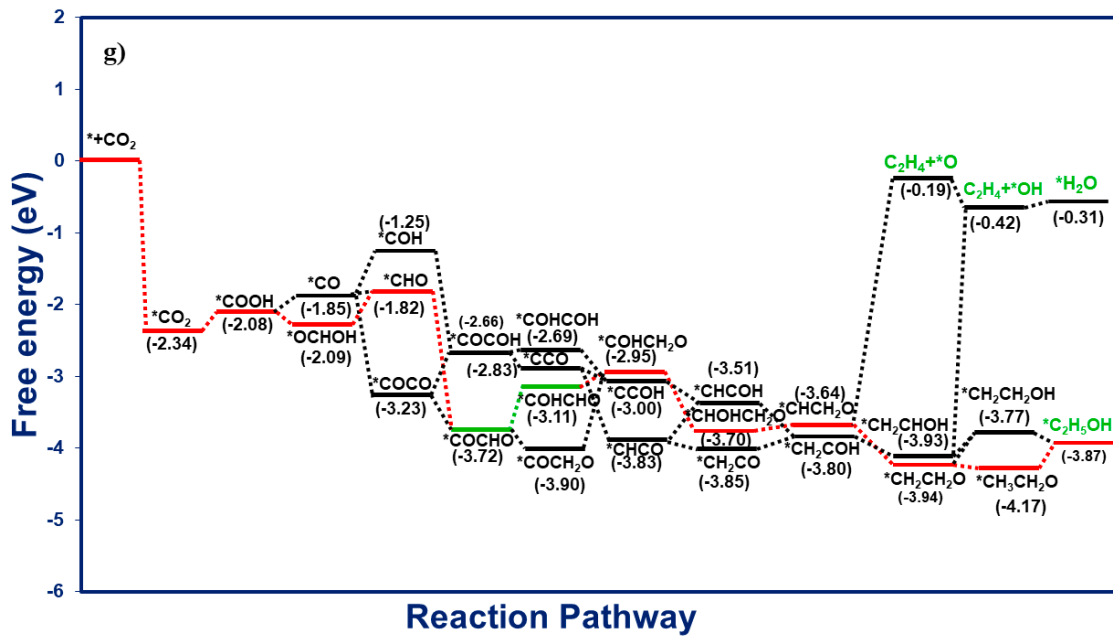
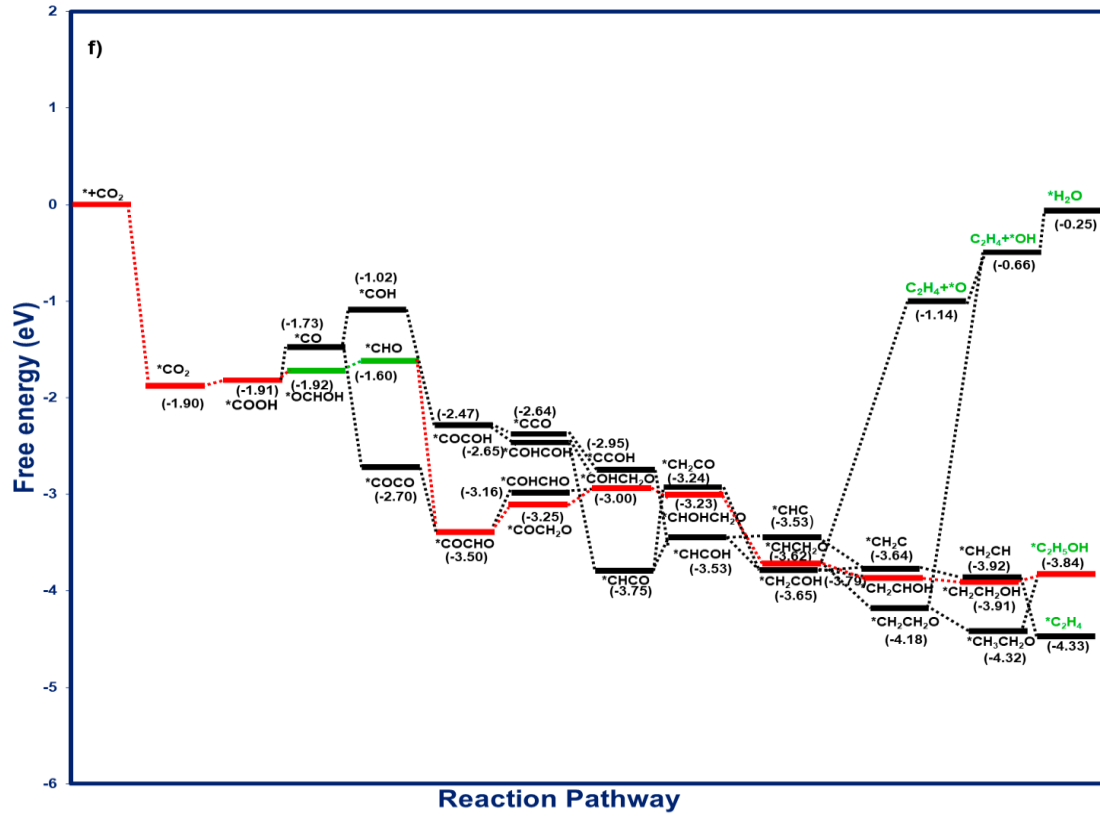


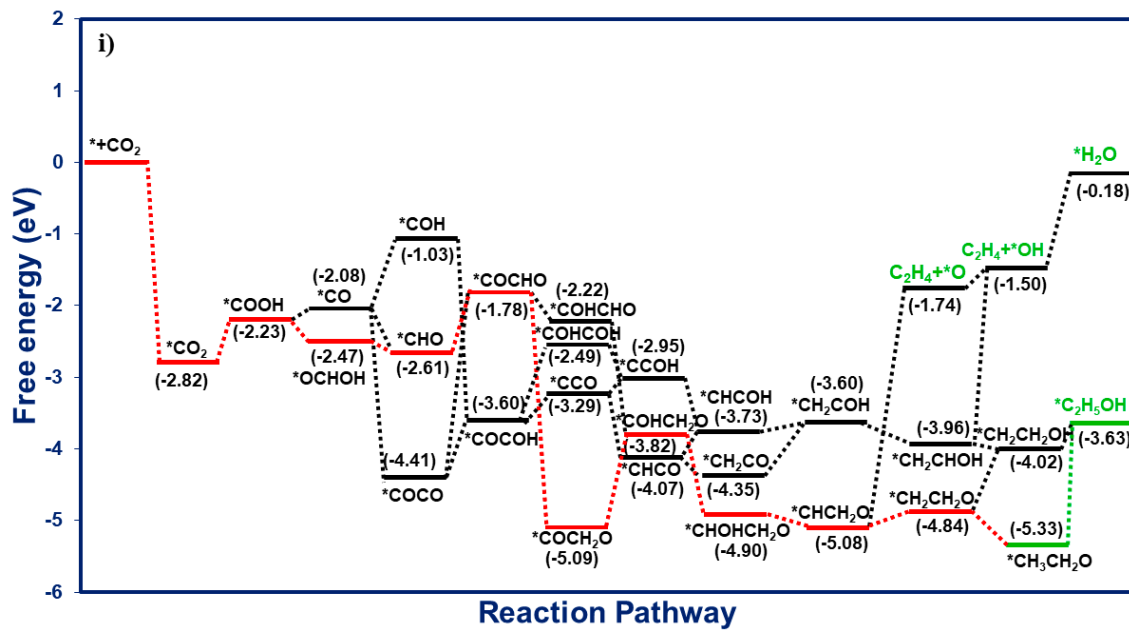
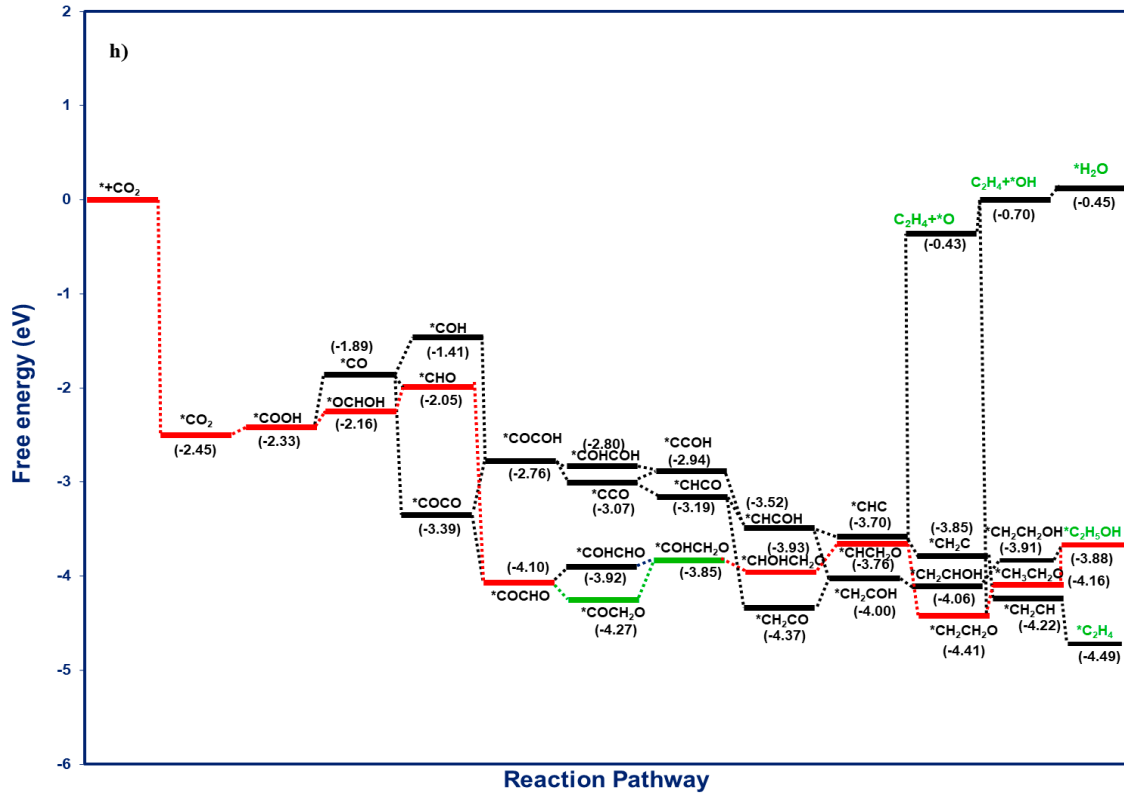
Fig. S5: Detailed computed free energy diagram representing the various possible pathways for the reduction of CO_2 to C_1 products on a) Cr_2NbC_2 b) Cr_2TaC_2 c) Cr_2TiC_2 d) Cr_2VC_2 e) Mo_2NbC_2 f) Mo_2TaC_2 g) Mo_2TiC_2 h) Mo_2VC_2 i) Ti_2NbC_2 j) Ti_2TaC_2 k) V_2TaC_2 l) V_2TiC_2 . The

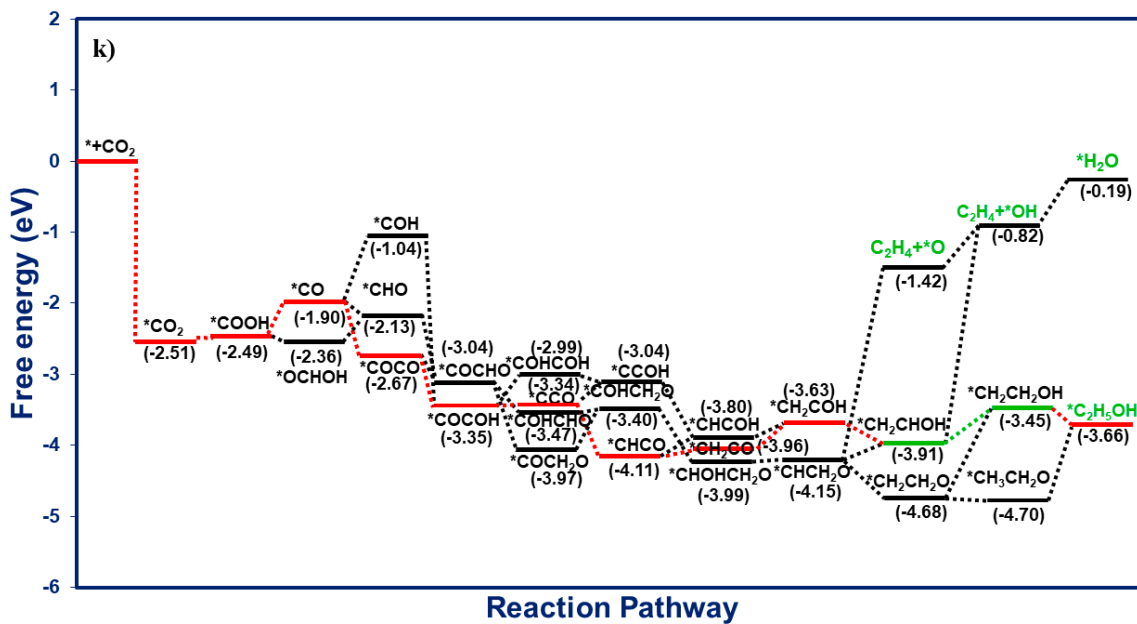
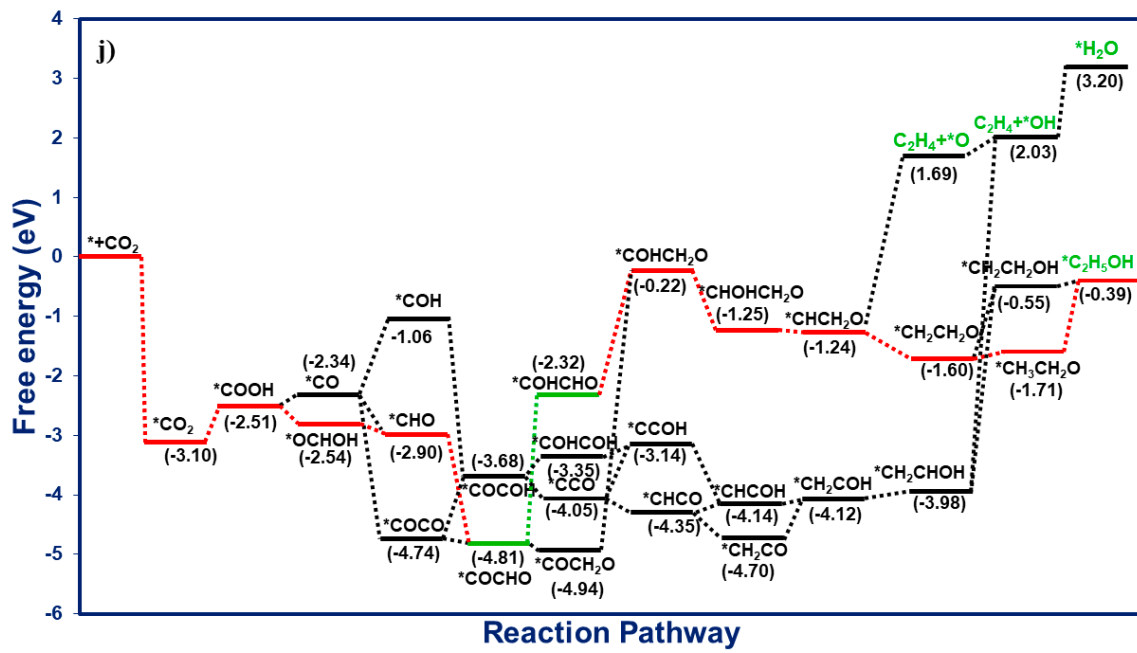
most favourable pathways are highlighted in red colour with the potential determining steps represented by green colour.











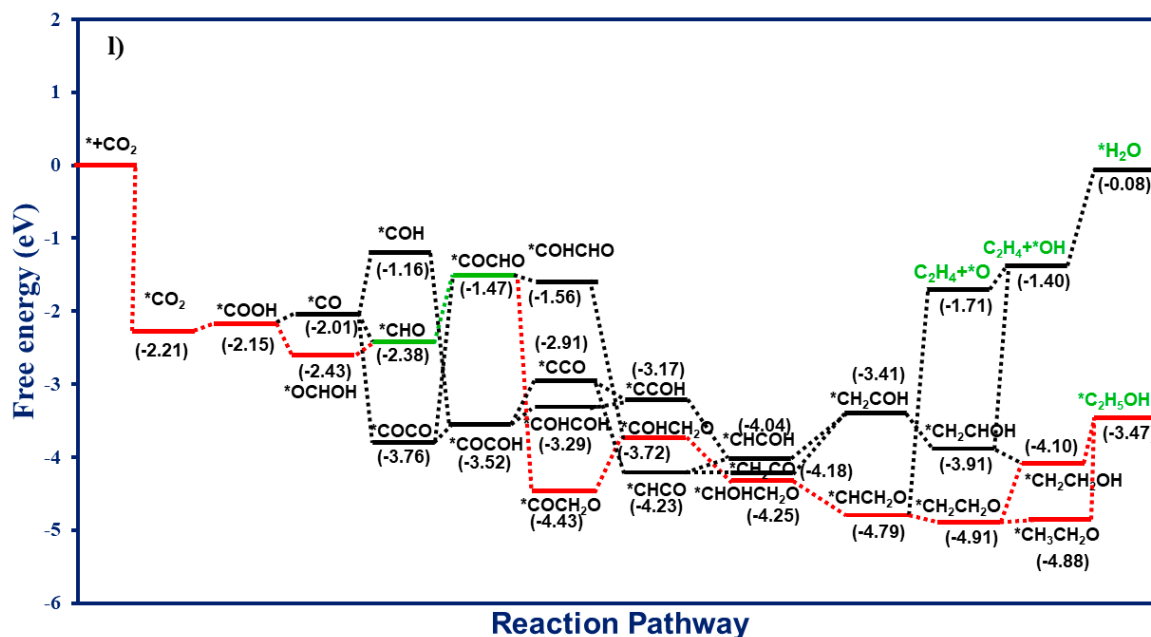


Fig. S6: Detailed computed free energy diagram representing the various possible pathways for the reduction of CO₂ to C₂ products on a) Cr₂NbC₂ b) Cr₂TaC₂ c) Cr₂TiC₂ d) Cr₂VC₂ e) Mo₂NbC₂ f) Mo₂TaC₂ g) Mo₂TiC₂ h) Mo₂VC₂ i) Ti₂NbC₂ j) Ti₂TaC₂ k) V₂TaC₂ l) V₂TiC₂. The most favourable pathways are highlighted in red colour with the potential determining steps represented by green colour.

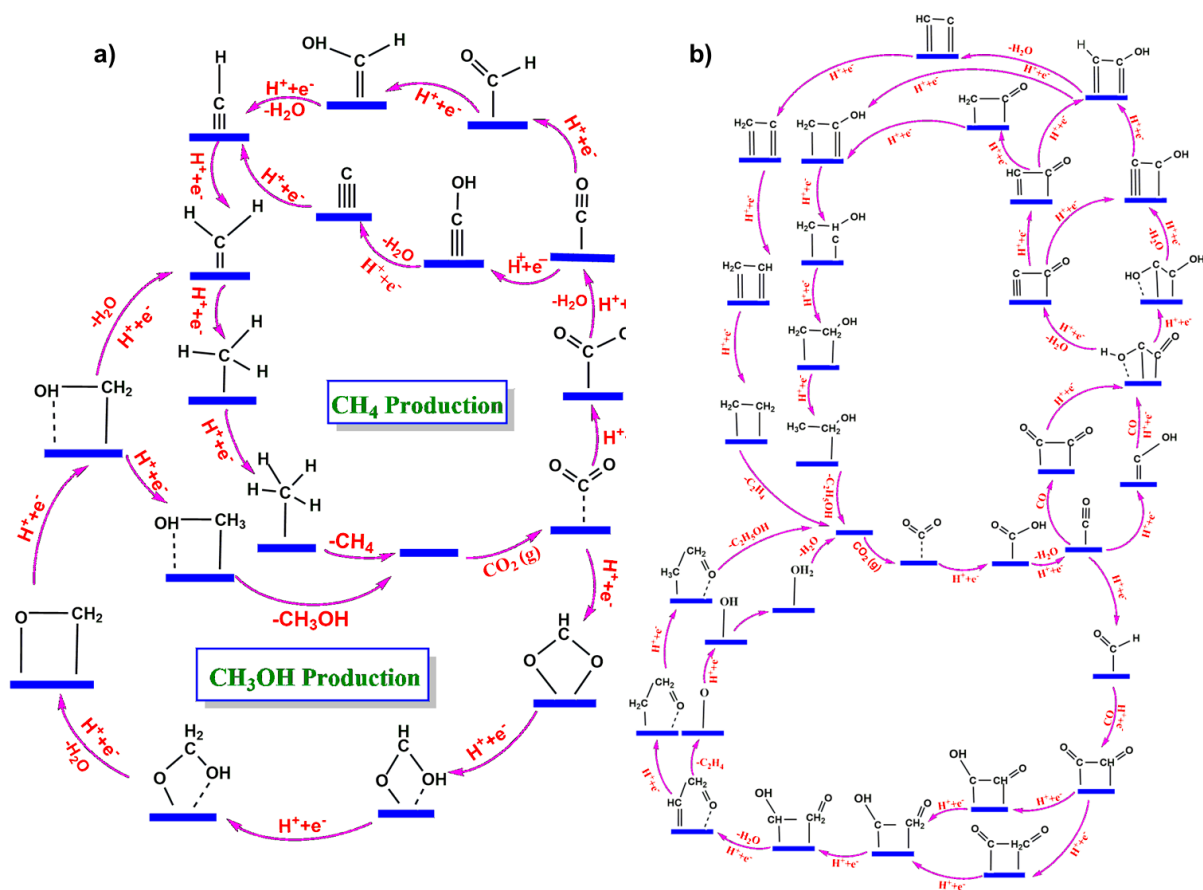


Fig. S7: Proposed reaction mechanism for CO₂ reduction to a) C₁ products (CH₄ and CH₃OH) and b) C₂ products (C₂H₄ and C₂H₅OH) on MXenes.

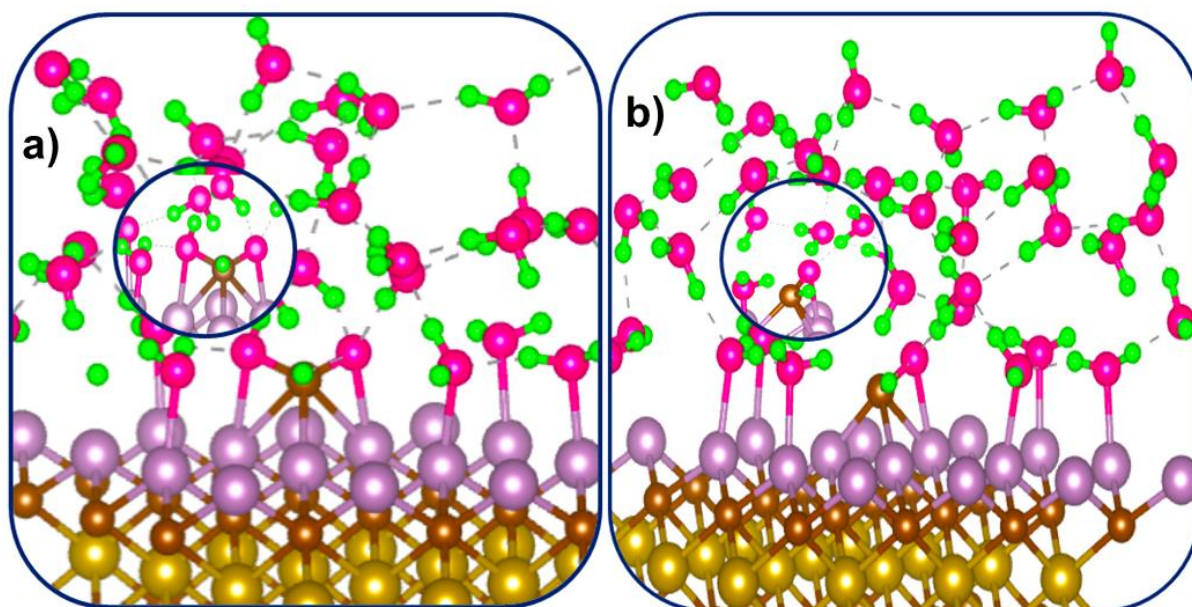


Fig S8: Electrode/Solution Interface of potential determining steps of CO₂ reduction on Mo₂TaC₂ MXene: a) Initial state and b) Final state of C₂ products.

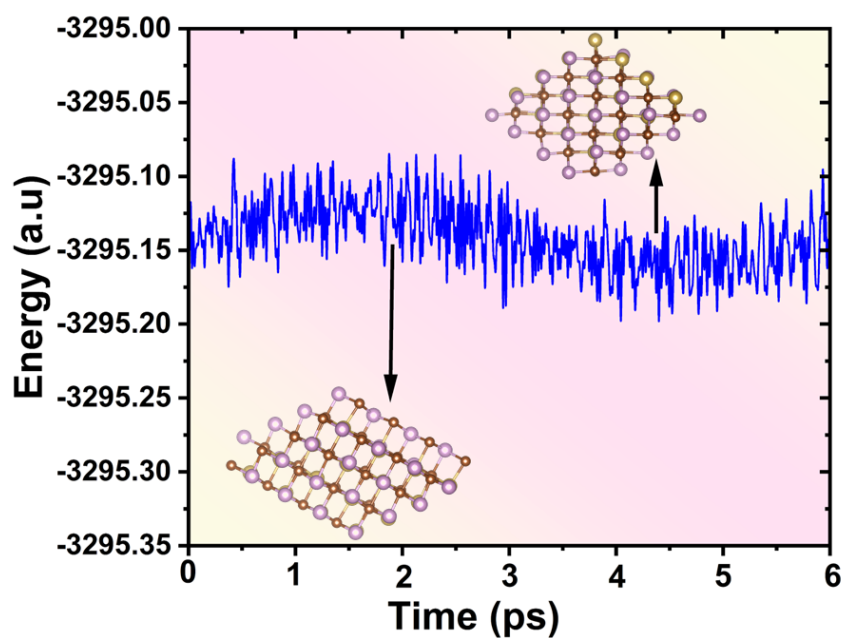


Fig. S9: Variation of energy versus the AIMD simulation time for Mo₂TaC₂ for 6 ps at 600 K. The insets are the top views of snapshots of configurations.